

Development of environment friendly electrical insulation from natural fibrils

Subhash Nimanpure^{1,2*}, S. A. R. Hashmi^{1,2}, Rajnish Kumar³, Archana Nigrawal⁴, H.N. Bhargaw^{1,2}, Ajay Naik²

¹Academy of Scientific and Innovative Research (AcSIR), India

²CSIR-Advanced Materials and Processes Research Institute, India

³Gautam Buddha University, Greater Noida, India

⁴Maulana Azad National Institute of Technology, India

*Corresponding author

DOI: 10.5185/amp.2018/805

www.vbripress.com/amp

Abstract

Environment friendly electrical insulation material was developed using bio based rectangular cross sectioned sisal fibrils as reinforcement. High content cellulose base fibrils fibrillated by mechanical disintegration method into macro and micro fibrils from coarse sisal fibre. These fibrils were randomly distributed in polymer matrix. These composites were characterized in term of electrical, mechanical and thermal properties to investigate the stability for high strength electrical insulation materials. Excellent mechanical properties were observed. Tensile, flexural and impact strength of composites at 40 wt. % fibril loading improved by 151.34, 197.43 and 360.07 % as compared to unsaturated polyester resin. A few micro-mechanical models were compared with the experimental values. Nielson-Chen Model predicted the experimental data most accurately. The electrical properties of surface modified sisal fibril composites improved significantly in higher frequency. DSC analysis showed that the decomposition temperature of composite was higher, around 22°C than that of the polyester resin. Thermal degradation reduced and was observed in the range of 83-87% of fibril composites as compared to 97% of resin. Fibril composites are highly sensitive to electrical frequency and exhibit excellent electrical insulation property at 20 kHz. Alkali treated fibril based composites resulted an environment friendly thermally stable, high strength insulation material. Copyright © 2018 VBRI Press.

Keywords: Sisal Fibril, sisal fibril bio-composites, electrical properties, mechanical properties, thermal properties.

Introduction

Polymer composites with organic fillers like cellulose based natural fibres have been receiving appreciable attention because of higher strength and issues concerning environmental pollution. These composites possess comparable mechanical properties with artificial fibres based composites [1, 2]. Natural fibre composite materials are widely used in building, automotive and packaging industries. However, their utilization in dielectric applications is comparatively rare phenomenon. These composites are being utilized as dielectric materials as a part of microchips, transformers, terminal, connectors, switches, circuit sheets etc. Renewable source based such composites need to be studied further to expand area of reliable, environ friendly green insulation dielectric materials. Different types of natural fibres like sisal, flax, jute, banana, hemp, ramie, coir, and pineapple leaf have been investigated for reinforcement [3-14]. Sisal fibre is one of the most promising natural fibres for application where the combination of electrical and mechanical properties is required [15]. The sisal fibre consists of 49-78% cellulose, 3-8% lignin, 10-24%, hemicellulose, 1-2% waxes and 0.1-1% ash by weight. The diameter ranges about 100–300 µm and length between 1 to 1.5 m.

Natural fibres possess complex hierarchic structure. A fibre is composed of a bundle of macro and micro fibrils. Micro-fibril is further composed of thousands of cellulose chains. Different mechanical properties can be obtained from natural fibres depending on the processing mechanism to yield the reinforcing materials. A drastic reinforcing outcome can be attained by fibrillation of plant fibres into micro-fibrils with small diameters [15]. In spite of excellent mechanical properties of sisal fibre, its application is limited to low value composite products because it is difficult to maintain a uniform and homogeneous fibre distribution in composites which is an outcome of stiffness and coarse diameter of sisal fibre. In order to overcome this limitation, in this work fibrillation of sisal fibres into macro and micro fibrils has been carried out by mechanical disintegration method to control variations in fibre distribution. As for the development of natural fibre polymer composites is concerned, the hydrophilic nature of natural fibres causes poor surface adhesion with the hydrophobic matrix and limits the potential use of natural fibres as reinforcing agent. Many researchers have used different surface modification strategies for the fibre surface modification and reported improvement in mechanical properties of the

resulted chemically treated composites [16-18]. The chemical treatment of fibre surface can selectively remove the less desired constituent present in the fibre, to improve overall effectiveness of reinforcement. Myslamy and Rajendran [17] reported that 5 % alkali treatment removes completely the hemicellulose from the sisal fibre leaving behind 86.27% cellulose, 4.05% lignin, 0.14% wax. Improved mechanical and water absorption resistance of alkali treated short fibre reinforced polymer composites was also reported [18]. Ghali et al. [19] reported that surface modification techniques such as alkali treatment with acetylation, increased mechanical properties and diffusion process. Aziz and Ansell [20, 21] observed that the alkali treated hemp fibre polyester composites showed superior mechanical strength. Singh et al. [22] reported that mechanical properties of sisal polymer composite increased due to the chemical treatment of fibre. The mechanical and electrical properties of natural fibre based polyester composites have been reported [23, 24]. The dielectric constant and mechanical strength of composites increased with fibre loading [25]. However, the dielectric constant of short sisal fibre reinforced LDPE composite, decreased as a result of chemical treatment [26]. The impact strength, flexural strength, and flexural modulus of sisal fiber cellulose microcrystal reinforced polyester composites found higher than those of unsaturated polyester resin by 41.08%, 52.52%, and 32.31%, respectively [27]. In another investigation alkali treated fibers improve the tensile strength (96%) and flexural strength (60%) of unsaturated polyester toughened epoxy network nanocomposite [28]. The dielectric insulation property of composites decreased with increase in volume fraction of fibre in the composites [29].

In present study, the fibrillated sisal fibre, in the form of loose sisal fibril was incorporated as reinforcing component in unsaturated polyester resin to develop environment friendly electrical insulating material having an enhanced combination of thermal and mechanical properties. This manuscript attempts to give an insight about the influence of fibrillated sisal fibre loading and alkali treatment on electrical, mechanical and thermal properties of sisal fibril reinforced polyester composite. The morphology of the composites was characterized using scanning microscopy.

Experimental

Materials

The sisal fibrils were obtained by mechanical disintegration process [30], according to which sisal fibres were processed in an industrial beater to convert the coarse fibres into fine fibrils in the form of pulp. Sisal pulp was transferred and spread on a sheet of cotton cloth over a wire mesh and was dried in the sun for 24 hours for complete removal of moisture to obtain the sisal paper having density 1.16 g/cm³. Sisal fibrils were separated from handmade sisal paper using fibre separation equipment which was designed in CSIR-AMPRI Bhopal for this purpose. The separated fibrils were used in the preparation of composites as reinforcement filler.

Unsaturated polyester resin was supplied by P.S. Associates, Industrial Area Govindpura, Bhopal, India. The density of this resin was 1.1 – 1.2 g/cm³. The viscosity at room temperature was 500 cps and monomer content was 35%. Cobalt naphthanate was used as accelerator and methyl ethyl ketone peroxide was used as catalyst. Sisal fibrils were separated from handmade sisal paper using fibre separation equipment which was designed in CSIR-AMPRI Bhopal for this purpose.

Alkali treatment (NaOH) on sisal fibrils

The sodium hydroxide (NaOH) was obtained from Rankem Avantor Performance Material India Limited, Panoli, Ankleshwar, Gujarat, India. A 5wt.% arrangement of sodium hydroxide was used for sisal fibril treatment. Sisal fibrils were immersed into the solution for 72 hours at room temperature then washed with running water for complete removal of NaOH. Fibrils were dried at 80°C temperature for 24 hours by utilizing air circulation oven for complete removal of moisture.

Preparation of composite

The sisal fibril reinforced polyester composites as defined in **Table 1** were developed by utilizing cold stage compression molding technique. The samples were designated as follows; untreated and treated sisal fibrils were denoted as US and TS respectively. After US / TS a number shows the wt. % of sisal fibril. Thereafter, polyester is denoted by P, followed by wt. % of polyester. Mild steel rectangular mold, having dimension of 120 mm × 120 mm × 15 mm was used. The teflon sheet was utilized for easy removal of samples from mold. Unsaturated polyester resin, accelerator and catalyst agent were weighed by required composition and were blended legitimately. The sisal fibrils were mixed with resin mixture for 15 minutes for proper coating of fibrils. The mixed material was uniformly spread over the wax coated mold surface. At last the mold was compacted by top punch plate and placed in between plates of hydraulic press with uniform pressure at room temperature. The polyester was set in 4 hours and composite sample was taken out from the mold. The composite plates were post cured at 120° C for 4 hours in an air circulation oven. The prepared specimens are shown in **Fig. 1**.



Fig. 1. Prepared specimens.

Table 1. Nomenclature

Designation	Composition		Alkali treatment of sisal fibril
	Sisal Fibril (g.)	Polyester Resin (g.)	
Unsaturated Polyester resin (Polyester)	Nil	100	N.A.
USF10P	10	90	Untreated
USF20P	20	80	Untreated
USF30P	30	70	Untreated
USF40P	40	60	Untreated
TSF10P	10	90	NaOH Treated
TSF20P	20	80	NaOH Treated
TSF30P	30	70	NaOH Treated
TSF40P	40	60	NaOH Treated

Characterization

Scanning Electron Microscopy (SEM) and Field Emission Scanning Electron Microscopy (FESEM)

The tensile fractured surface of different wt. % composites were observed and compared by using Scanning Electron Microscope (SEM), Model No. JEOL JSM-5600. All specimens were sputtered with 10 nm layer of gold before SEM observations. Every specimen was mounted on the holder of the microscope using double sided conduction carbon adhesive tape. The voltage rating of 2–10 kilovolts was used for SEM observation.

The field emission scanning electron microscope (FE-SEM) characterization was done by using NOVA NANOSEM 430, m/s FEI, USA. The flexural fractured surfaces of different composites were analyzed by using FE-SEM. The sputtering process of specimen was same as SEM. The accelerating voltage of about 5 -10 kilovolts was employed in the operation of FE-SEM.

Mechanical characterization

Tensile tests were carried out according to ASTM D 3039. The test were carried out by using Instron UTM, Model No. 8801, equipped with 100 kN load. The three tensile specimens were tested of each sample. The size of the test specimen was 120 mm x 15 mm x 3 mm. The cross head speed was 2 mm/min. The flexural tests were carried out according to ASTM D 790-30 at room temperature using UTM TINIUS OLSEN H25KT, 25 kN load capacity with cross head speed 10 mm/min. Three specimens of each sample were tested. The dimension of each specimen was 70 mm x 15 mm x 3 mm. The span length was 50 mm with span to thickness ratio more than 16:1. The impact test was done according to standard

ASTM D 256-05 at room temperature, by manually operated CEAST Izod pendulum impact tester. Three specimens of each sample were tested. The dimension of each specimen was about 60 mm x 12.7 mm x 3 mm with notch of 2.54 mm.

Electrical characterization

Dielectric constant (ϵ') was evaluated by using the following relation

$$\epsilon' = C/C_0 \quad (1)$$

where C and C_0 are the capacitance values of specimen and air respectively;

C_0 is given by $[(0.08854 A)/d]$ pF,

where A (cm²) is the area of the electrodes and d (cm) is the distance between electrodes. Capacitance (C) of the samples was measured at room temperature and frequency range from 1 to 20 kHz by using a Hewlett - Packard, LCR Meter, model 4274 A.

Dissipation factor $\tan \delta$ is reciprocal of ratio between the insulating material capacitive reactance to its resistance at specified frequency and is defined as

$$\tan \delta = \epsilon''/\epsilon' \quad (2)$$

where ϵ'' is the dielectric loss.

AC conductivity of the samples was calculated by using the following relation,

$$\sigma_{ac} = \epsilon_0 \omega \epsilon' \tan \delta \quad (3)$$

ϵ_0 is permittivity of material in free space, ω is the angular frequency, which is equal to $2\pi f$ (f is the frequency).

Thermal characterization

The thermal behavior of composites was observed by thermo-gravimetric analysis (TGA) and differential scanning calorimetry (DSC) techniques. The different wt. % composites were analyzed using Mettler Toledo thermal analyzer Linseis, Germany, Model No. DSC 1. The heating rate of machine was 5 °C with temperature range of 20 to 500 °C for DSC and 20 to 600 °C for TGA analysis.

Results and discussion

Scanning Electron Microscopy and Field Emission Scanning Electron Microscopy

The **Fig. 2a** shows the morphology of the coarse sisal fibre along with the bundles of macro and micro sisal fibrils. The diameter of the coarse sisal fibre was observed about 80-150 μ m. The process of conversion from fibre to fibril has been discussed earlier in experimental as materials. The **Fig. 2b** shows the morphology of untreated sisal fibrils. Fibrils are semi rectangular in shape, having traces of wax coating over the surface. The width of sisal fibril was observed about 5–20 μ m. The cross sectional area of sisal fibril fracture is shown in **Fig. 2c**. The fractograph of NaOH treated sisal fibril is shown in

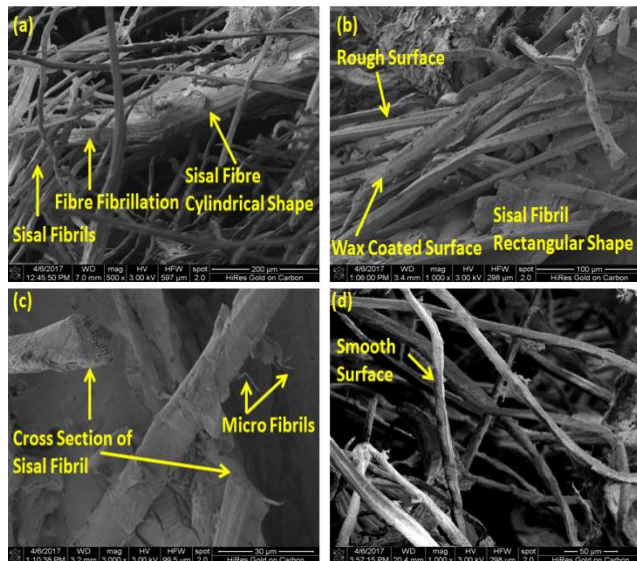


Fig. 2. FESEM Morphology (a) coarse sisal fibre (b) untreated sisal fibrils (c) cross sectional area (d) NaOH treated sisal fibril.

Fig. 2d. The surface of NaOH treated sisal fibril is smooth having less traces of wax as compare to untreated sisal fibril, having a uniform cross section.

The tensile fractured specimens were used for SEM observation. The fractured surfaces of polyester, untreated and alkali treated sisal fibril polyester composites are shown in Fig. 3a-c. The fractured surface of the polyester sample is reported in Fig. 3a. The surface shows the typical morphology of a brittle polyester matrix. The Figure 3b, reports the fracture surface SEM micrograph of the USFC. Rough surfaces were visible which contains maximum amount of fibril pullout throughout the composite and poor bonding between fibril and matrix. The sisal fibril was partially dispersed with polyester, demonstrating weak fibril matrix interlocking and indicating poor fibril matrix adhesion. In Figure 3c for the same weight fraction of TSFC, the better adhesion was observed between fibril and polyester matrix, indicating the strong fibril matrix interlocking. The alkali treatment leads to further fibrillation. Therefore, it increased the effective surface area for adhesion of fibril and matrix. Alkali treated fibrils were more uniformly distributed as compared to untreated fibril. The morphology and sisal fibril distribution in polyester composites are shown in Fig. 4a-b. Fig. 4a, illustrates a composite having 30 wt. % fibrils loading whereas Fig. 4b, illustrate 40 wt. % fibrils loading. Fibrils and polyester matrix can be seen in this micrograph. Variation in loading, length, straightness of fibrils is visible. The fracture pattern of polyester is brittle however, the composite moving towards ductile with increased content of sisal fibrils. The SEM analysis shows that bonding between treated fibril and polyester is superior as compared to the untreated fibril and polyester. The untreated fibril seems to be free of matrix material and shows the poor fibril matrix interlocking. However, treated fibril shows good mechanical interlocking and responsible for increased strength of composites.

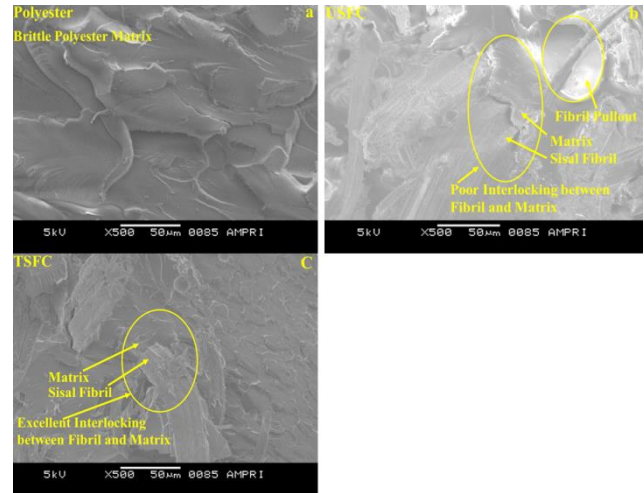


Fig. 3. SEM fractographs (a) Polyester (b) USFC (c) TSFC.

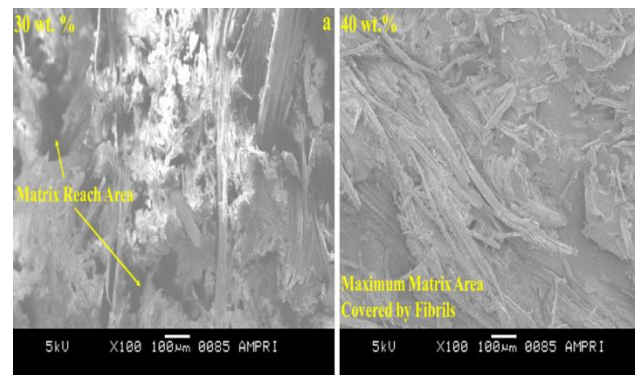


Fig. 4. SEM fractographs- effect of higher sisal fibril loading on composites (a) 30wt. % sisal reinforced polyester composites (b) 40wt. % sisal reinforced polyester composites.

Table 2. Variation in tensile strength of fibre.

Fibre Category	Tensile Strength(MPa)
Coarse sisal fibre	400-600 MPa
Sisal fibril	650-780 MPa
NaOH treated sisal fibril	800-850 MPa

Mechanical characterizations

Fibrillation of course sisal fibre to fine fibrils resulted in significant improvement in terms of tensile strength as shown in the Table-2. Refinement of the fibre influences its tensile strength [31]. A decrease in fibre fineness results in higher fibre strength. Fibrillation of course fibres into fibrils results in decrease in number of defects present in the cross-section thus improves the tensile strength. The defects are primarily the voids present in the weak bonding material of the cells. NaOH treatment sisal fibrils showed significant improvement in tensile strength as compared untreated sisal fibril. NaOH treatment leads to removal of lignin and hemicellulose present in the fibrils enhancing its tensile characteristics. Removal of hemicellulose results in the reduction of density and rigidity of the interfibrillar region and thus enables the fibrils more capable of rearranging themselves along the

direction of tensile deformation [32]. In stretched condition, rearrangement results in better load transmitting capacity among the fibril, hence higher stress bearing capability. Lignin removal causes the middle lamella to become more plastic and homogenous due to elimination of micro-voids, improving the tensile characteristics of the fibril.

The variation in tensile strength and modulus of pure unsaturated polyester resin and varying sisal fibril loading for untreated sisal fibril polyester and alkali treated sisal fibril polyester composites are shown in the Fig. 5 and Fig. 6. From Fig. 5 shows that tensile strength of polyester resin increases after its reinforcement with untreated as well as surface modified alkali treated sisal fibril. Polyester specimen was found to bear a maximum tensile strength 29.35 MPa, whereas composites with untreated sisal fibril of 10, 20, 30 and 40 wt. % exhibited tensile strength of 38.43, 46.45, 50.16 and 51.12 MPa respectively. Further it was observed that the tensile strength of composites having treated fibril increased. The polyester matrix when reinforced with alkali treated sisal fibrils of 10, 20, 30 and 40 wt. % was found tensile strength of 49.94, 58.29, 68.04 and 73.77 MPa respectively. The most significant improvement in tensile strength was observed as 30.93 % in case of 10 wt. % untreated fibril loading and 70.15 % in case of 10 wt. % treated fibril loading as compared to polyester resin. The maximum improvement in tensile strength of TS40P60 composite was observed as 151.34 % than polyester resin and as 44.30 % than US40P60. From Fig. 6, the modulus of polyester and US40P60 composite were 1.83 GPa and 3.73 and that of TS40P60 composite was 4.54 GPa. The modulus of TSF40P composite was increased 148.03 % than modulus of polyester resin and 21.66 % than modulus of USF40P composite. NaOH treatment of the sisal fibrils removed hemicellulose and in turn increased the content of cellulose in the fibre that enhanced the strength of fibre [31]. Alkali treated sisal fibril improved the tensile strength as well as modulus that may be attributed to the improved adhesion between the fibril and polymer matrix. The increase in tensile strength with the increased loading of sisal fibril, clearly indicates the effective reinforcement of fibres. The increase in tensile strength of composites having treated fibril as compared to untreated fibril composites, one may be attributed to fact that NaOH treatment improves the adhesive characteristics of fibril surface by removing natural and artificial impurities thereby producing a rough surface morphology[33]. Additionally, NaOH expands the strong surface range accessible for contact of fibril with matrix in this manner offers a superior fibre/matrix interface and increases the tensile strength. In case of untreated fibril, OH groups on fibril surface make the fibril as a hydrophilic nature with hydrophobic polyester matrix which at last results in poor fibre/matrix interfacial bond and lower tensile strength. It has been seen that composites with 40 wt. % reinforcement indicated better tensile strength and modulus for both untreated and treated fibril reinforced polyester composites and results were much superior for alkali treated sisal fibril.

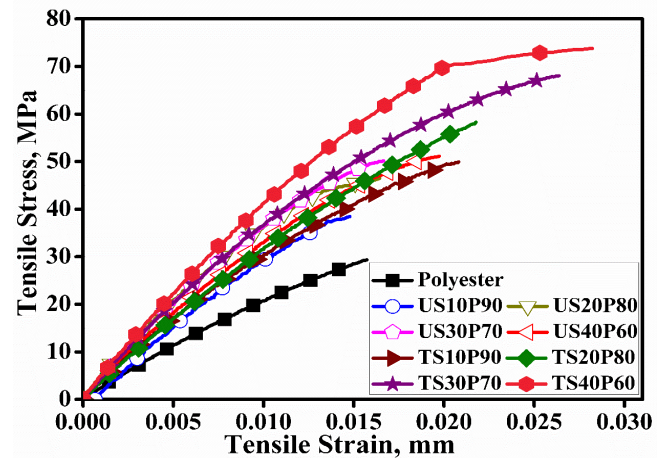


Fig. 5. Tensile strength of Polyester, USFC and TSFC with variation of sisal fibril loading.

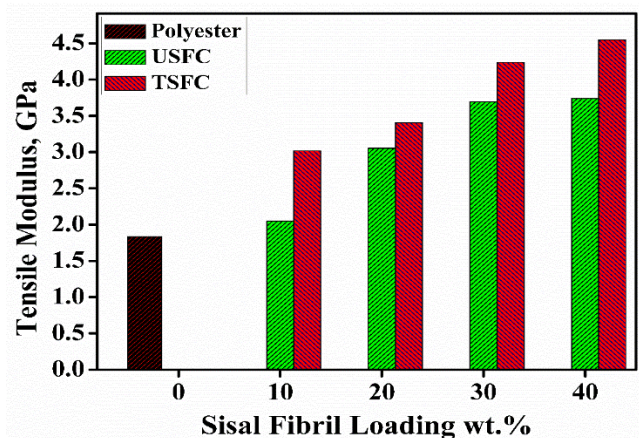


Fig. 6. Tensile modulus of Polyester, USFC and TSFC with variation of sisal fibril loading.

The flexural strength and modulus of composites with treated as well as untreated fibril have been depicted in the Fig. 7 and Fig. 8. In these graphs similar trends were observed as tensile strength and modulus. The flexural strength of composites with treated fibrils was higher than that of untreated fibrils composites. It was noticed in Fig. 7, that flexural strength increased with respect to increase in fibril loading up to 30 wt. % and then slightly increases with further increase in fibril loading across the both treated and untreated composites. The flexural strength of polyester, US40P60, and TS40P60 specimens were 38.98, 94.42, and 115.94 MPa respectively. Thus, the flexural strength of TS40P60 composite was 197.43 % more than that of polyester resin and 22.79 % more than US40P60 composite. Increase in loading of fibril in the composites from 10 to 30 wt. %, increased the flexural strength from 51.00 to 90.80 MPa for untreated sisal fibril composites (USFC) and 73.29 to 99.14 MPa for treated sisal fibril composites (TSFC) respectively. The flexural modulus showed the similar trend as tensile modulus. From Fig. 8, the flexural modulus of polyester, US40P60 and TS40P60 were measured 2.22, 3.12 and 4.50 GPa respectively. The increase in fibril loading in USFC and TSFC composites

from 10 to 30 wt. %, the modulus changed from 2.41 to 3.07 and 3.07 to 3.81 GPa respectively. The flexural strength as well as flexural modulus increased in the treated composites showing better adhesion between fibril and matrix material and the better wetting of surface modified fibrils with polyester matrix in comparison to untreated fibrils.

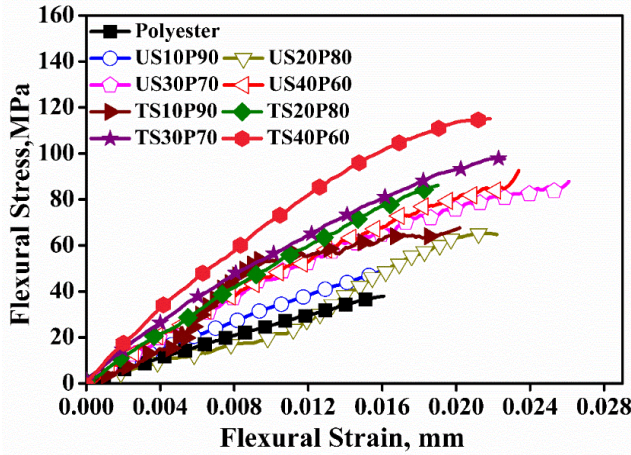


Fig. 7. Flexural strength of Polyester, USFC and TSFC with variation of sisal fibril loading.

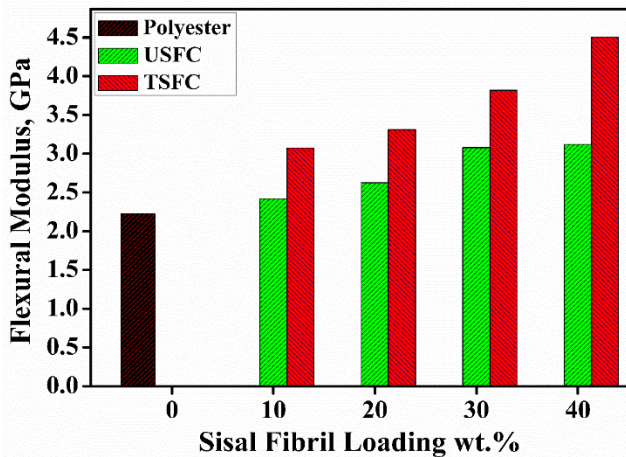


Fig. 8. Flexural modulus of Polyester, USFC and TSFC with variation of sisal fibril loading.

The effects of surface modifications on the impact strength of the USFC and TSFC have been depicted in Fig. 9. It was observed that the TSFC have higher impact strength than that of USFC composites. Similar trends were observed for tensile and flexural strength. Increasing the sisal fibril loading in the USFC and TSFC composite from 10 to 30 wt. %, the impact strength increased from 2.55 to 4.51 kJ/m² and 3.20 to 6.93 kJ/m² respectively. The impact strength of TS40P60 composites was observed as 7.58 kJ/m² as compared that of US40P60 composites as 6.14 kJ/m². The impact strength TS40P60 increased by 23.55% as compared to US40P60. The increased impact strength was attributed to NaOH treatment which improved the fibril surface adhesion characteristics by removing natural and artificial impurities [33]. The impact response of fibre composites

was influenced by the adhesive bond strength, fibre and matrix properties [34].

Micromechanical models

The elastic properties of natural fibre reinforced composites can be estimated from various micromechanical models. Properties such as Young’s modulus (E), Poisson’s ratio (ν) and volume fraction of both fibre and matrix are used to predict the properties of the composite material. In this research following models were used to predict the Young’s modulus of the studied material.

Rule of mixtures (ROM): Rule of mixture [35] predicts elastic properties of the composite material. The young’s modulus E₁ of composite is given by equation-

$$E_1 = E_F V_F + E_M V_M \tag{4}$$

E_F, E_M, V_F and V_M are Young’s moduli and volume fractions of the fibre and matrix materials.

Halpin – Tsai Equations: The Halpin-Tsai model [36, 37] was proposed by Halpin and Kardos, which was originally based on the Hill micromechanical model. This model is used to predict the elastic properties of the composite materials as per following relations-

$$P/P_m = \frac{1 + \xi \eta V_r}{1 - \eta V_r} \tag{5}$$

$$\eta = \frac{(P_r/P_m) - 1}{(P_r/P_m) + \xi} \tag{6}$$

P = composite properties (E₁₁, E₂₂, G₁₂, G₂₃), P_r = Reinforcement properties (E_r, G_r), P_m = Matrix properties (E_m, G_m), ξ = A measure of reinforcement geometry, packing geometry and loading conditions, V_r=Reinforcement volume fraction, ξ Factor is obtained by comparing the Halpin-Tsai equations with numerical solution of Micromechanics equations.

$$\xi = 2 l/t + 40 V_r^{10} \text{ for } E_{11} \approx \xi = 2(l/d) \tag{7}$$

40 V_r¹⁰ is a very small value.

For circular fibre- $l = l_f$ and $t = w = d_f$

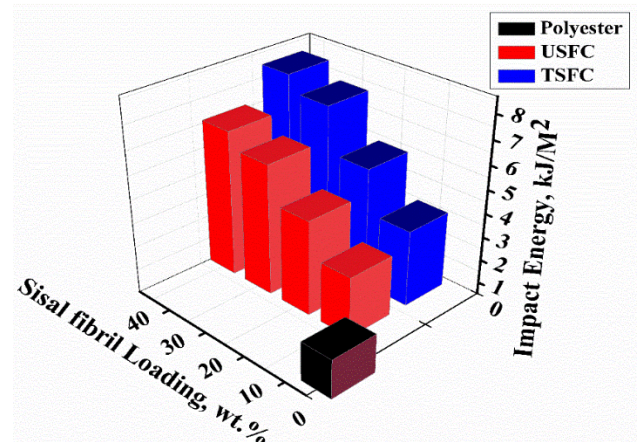


Fig. 9. Impact strength of Polyester, USFC and TSFC with variation of sisal fibril loading.

Nielson-Chen Model: Nielson-Chen model^[38] predicts the elastic properties of random fibre reinforced composites. The equation is expressed as follows.

$$E_c = \left(\frac{3}{8E_1}\right) + \left(\frac{5}{8E_2}\right) \quad (8)$$

$$E_1 = E_f V_f + E_m [1 - V_f] \quad (9)$$

$$E_2 = \frac{E_f E_m}{E_f [1 - V_f] + V_f E_m} \quad (10)$$

V_f – Fibre volume fraction

E_m, E_f – Modulus of matrix and fibre

E_c – Modulus of composite

Approximation Model by Manera: Another model proposed by Manera [39] predicts the elastic properties of randomly oriented short glass-fibre composites. The invariant properties of composites defined by Tsai and Pagano were used along with Puck’s micromechanics formulation. Manera simplified Puck invariants equations and the approximate equations can be expressed as follows.

$$E_c = V_f (16/45 E_f + 2 E_m) + 8/9 E_m \quad (11)$$

V_f – Fibre volume fraction

E_m, E_f – Modulus of matrix and fibre

E_c – Modulus of composite

Young’s moduli of composites with different sisal fibril loading (10 to 40 wt. %) obtained by experimental method were compared with the predicted values derived from different micro-mechanical models as shown in **Fig. 10** and average relative error between them was calculated. Rule of mixture (ROM) showed the maximum deviation from the experimental data with an average relative error of 33.43%. Modulus predicted by ROM was higher than the experimental modulus. Halpin-Tsai model showed an average relative error of 32.90%. The relative percentage error increased with fibre loading in the composite. Rule of mixture and Halpin-Tsai model showed almost similar results for the samples. Approximation model by Manera predicted the Young’s modulus with 9.88% average relative error. The relative error of 5.71% was found for 20% fibre loading composite which then increased with increasing fibre loading conditions. Nielson-Chen model showed an average relative error of 5.17% from the experimental values and was found to be most accurate among all the models. The average relative error decreased with fibril loading and showed relative error of just 0.107% for 40% by weight fibril loading. Nielson-Chen used theory of elasticity approach to predict the modulus of randomly oriented fibre composites. To determine the mechanical properties of composite with any fibre distribution, an averaging technique, along with micro-mechanical equations and transformation equations was used giving geometrically averaged value for the entire range of fibre angles. The geometrically averaged Young’s modulus is assured to be same as the in-plane Young’s modulus of the isotropic composite. Thus, predicting the Young’s modulus for random fibre composites most accurately.

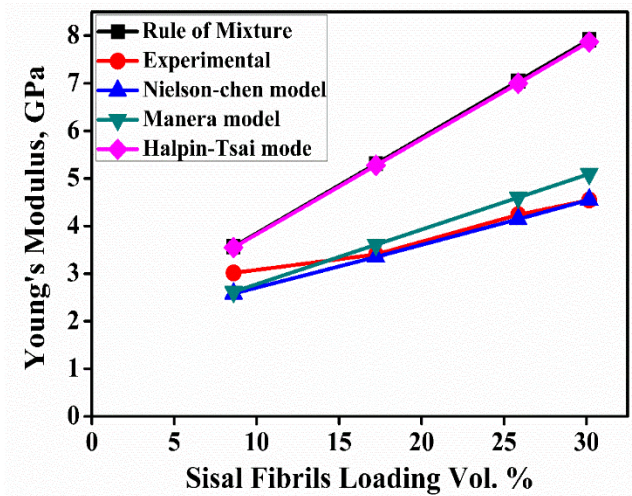


Fig. 10. Micro-mechanical models of composites with the variation of sisal fibril loading.

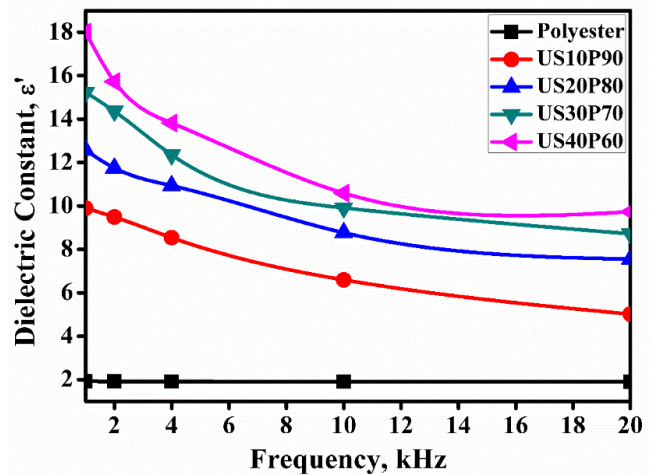


Fig. 11. Dielectric constant of USFC with the variation of sisal fibril loading.

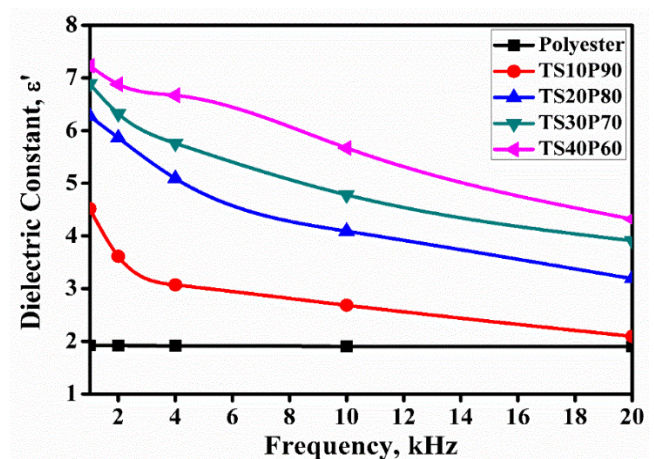


Fig. 12. Dielectric constant of TSFC with the variation of sisal fibril loading.

Electrical characterizations

The dielectric constant, dissipation factor and dielectric loss for polyester and both USFC and TSFC were measured at room temperature. **Fig. 11** and **Fig. 12** show

that the variation in dielectric constant (ϵ') with frequency for the untreated and alkali treated composites respectively at room temperature. The increase in loading of sisal fibril increased the dielectric constant of composites significantly. A diminishing value of dielectric constant was noticed with increased frequency. Sisal fibril reinforced polyester composites show higher sensitivity with change in frequency, as compared to polyester resin as shown in **Fig. 11**. Alkali treated fibril composites have low dielectric constant values than the untreated ones, as shown in **Fig. 12**. Hence, it could be inferred that TSFC exhibit good electrical insulation properties. As compared to polyester resin, the sisal fibril polyester composite were highly sensitive to change in frequency. The slope of the curves increased significantly in **Fig. 12** as compared to **Fig. 11**. This indicates the influence of alkali treatment on sisal fibrils that affected the trend. A sample containing 10 wt. % of treated sisal fibril at 10^3 Hz frequency has ϵ' value of 4.51 whereas specimen containing untreated sisal fibril of same wt. % loading has value of ϵ' as 9.89, that is more than double to the corresponding value of USFC. Further rise in frequency from 10^3 to 20×10^3 Hz, the value of dielectric constant of polyester, US10P90 and TS10P90 were observed 1.90, 5.01 and 2.09 respectively. It was noticed that the dielectric constant of TS10P90 composites is very close to dielectric constant of polyester. Dielectric constant of fibril reinforced composites was a little bit higher than polyester resin. This may be attribute to hydrophilic nature of natural fibre^[40].

The reduction of the value of ϵ' in alkali treated composites may be attributed to the removal of impurities such as wax and hemicellulose from the sisal fibril, due to increased hydrophobicity of the treated sisal fibrils than decrease in orientation polarization i.e., decrease in the percentage of moisture content in the sisal fibril. As a result, the dielectric constant of the fibril composites containing alkali treated fibril is lower than those of the untreated fibril composites. The decrease of dielectric constant in treated composites is also due to the increased interfacial adhesion between the fibril and the polyester matrix and chemical bonding caused in between them. Paul et al. ^[26] has reported that the treatment of filler material may change the structure of reinforced filler and hence responsible for the change in dielectric constant of composite. They also observed that dielectric constant of sisal fibre-low density polyethylene composite increased with increase in fibre loading. The increase was higher at low frequency and lower at high frequency, which was explained by considering the interfacial polarization and orientation polarization.

Dissipation factor ($\tan\delta$) of an insulation material is a very important parameter because it is used to measure the electrical energy loss across the material, which was converted to heat in an insulator. This parameter is used in selection of dielectric material for designing and manufacturing of required value of capacitor to be used in capacitor banks. **Fig. 13** shows that the variation in $\tan\delta$ with frequency for polyester and untreated sisal fibril

polyester composites at room temperature. With increasing frequency, the value of $\tan\delta$ was decreased for all the specimens.

The value of $\tan\delta$ of composites were increased at low frequency region and decreased at high frequency region for both type of composites. It was attributed to the free movement of dipoles within the material. As fibril loading increased across composite, the number of polar groups present in the fibrils were also increased which gave rise to increase in orientation polarization this resulted in an increase in dissipation factor values. Further at higher frequency region the orientation polarization disappeared and the value of $\tan\delta$ of composites decreased. The similar trends about relation between dissipation factor and frequency for alkali treated sisal fibril polyester composite were observed as shown in **Fig. 14**. An important observation was noticed in **Fig. 14** as compared to **Fig. 13**, where in particularly at low frequency region dissipation factor was very high for specimen which were prepared using alkali treated sisal fibrils.

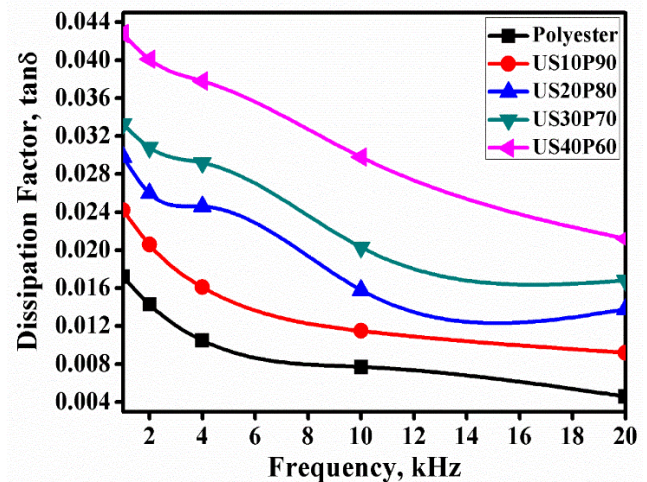


Fig. 13. Dissipation factor of USFC with the variation of fibril loading.

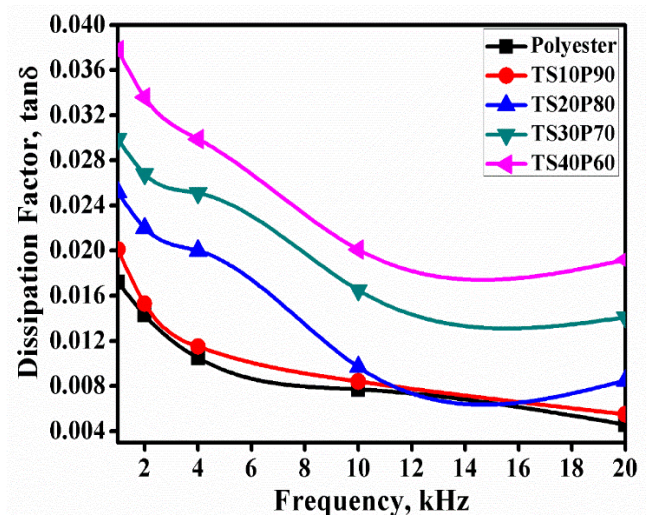


Fig. 14. Dissipation factor of TSFC with the variation of sisal fibril loading.

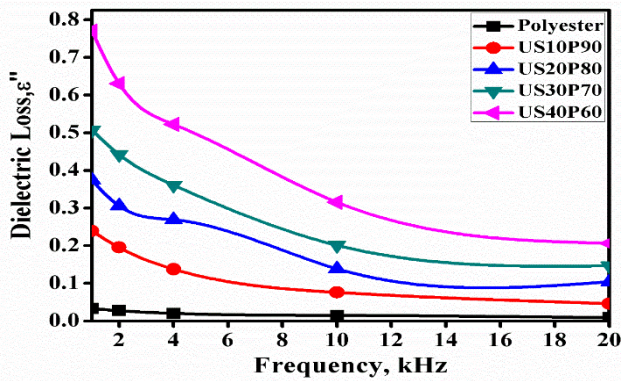


Fig. 15. Dielectric loss factor of USFC with the variation of sisal fibril loading.

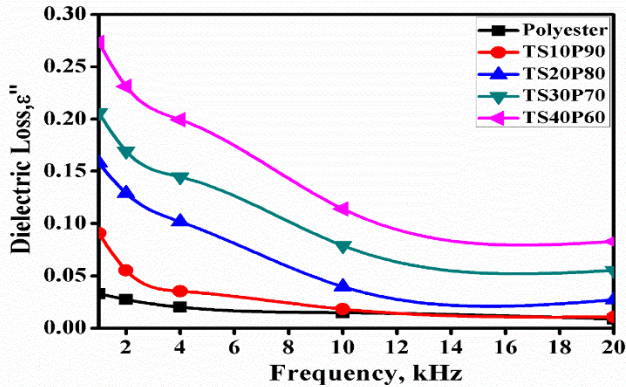


Fig. 16. Dielectric loss factor of TSFC with the variation of sisal fibril loading.

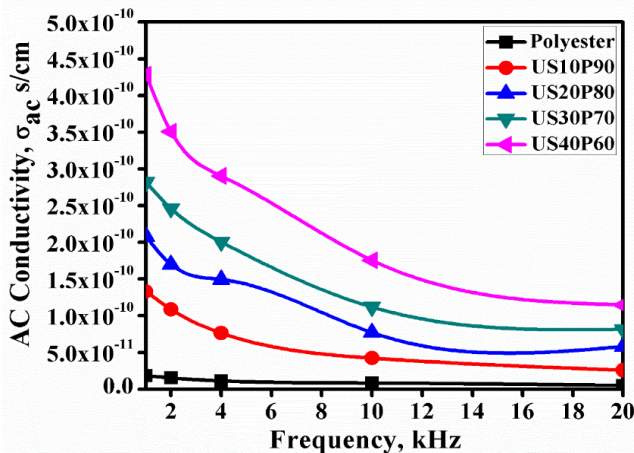


Fig. 17. AC conductivity of USFC with the variation of sisal fibril loading.

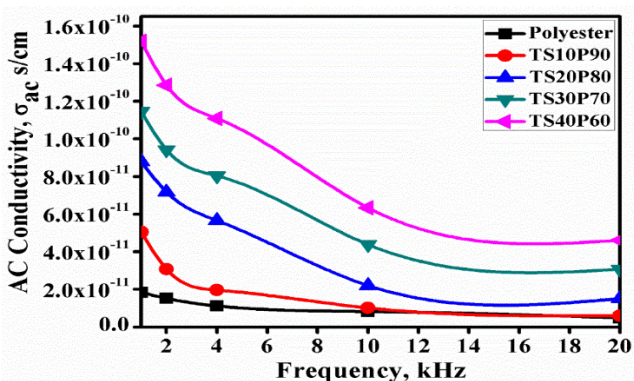


Fig. 18. AC conductivity of TSFC with the variation of sisal fibril loading.

Dielectric loss factor is utilized in electrical power transmission system as the average power factor for particular period of time. This factor helps in electrical power factor improvement of an electric system installation as it facilitates reduction of electrical energy losses in power transmission lines. The variation in dielectric loss (ϵ'') for the USFC and TSFC as a function of frequency are given in Fig. 15 and Fig. 16 respectively. It can be seen that in the lower frequency region, the dielectric loss was high and was higher for the composites having higher fibril content. As the frequency increased, the dielectric loss decreased rapidly and the slope of the curve increased. It indicates that in the lower frequency region, the dielectric loss depends upon the fibril content due to polarization of the fibrils, which was absent at higher frequencies. As the fibril loading increased, the heterogeneity of the composite increased, and hence increased its polarization that increases the dielectric loss in the composites.

The variations of the AC conductivity as function of the frequency for USFC and TSFP with different wt. % fibril loading at room temperature are shown in Fig. 17 and Fig. 18. These plots show that the AC conductivity increased with fibril loading and decreased with increasing frequency. The AC conductivity of US10P90 was observed as 1.33×10^{-10} S/cm at room temperature for 10³ Hz. Further rise in fibril loading from 10-40 wt. % in the composite, the AC conductivity of US40P60 was observed as 4.28×10^{-10} S/cm at room temperature for 10³ Hz. Similar rise in frequency from 10³ to 20x10³ Hz, The AC conductivity of US10P90 and US40P60 composites were observed 2.56×10^{-11} and 1.14×10^{-10} S/cm respectively. Similar trend was observed in case of TSFC. After the alkali treatment, the sisal fibril was free from the hemicellulose which may be responsible for increase the AC conductivity of composites. Thus, the results were superior with alkali treated sisal fibril composites. The AC conductivity of USFC and TSFC are excellent at higher frequency than lower frequency region due to reduction in polarization and ionic conduction of sisal fibril. The AC conductivity of polyester and its reinforced composites increased slightly with increase in sisal fibril loading that is attributed to hydrophilicity nature of sisal fibrils. This behavior also suggests that the electrical conduction increases at the higher loading of sisal fibril, which may be due to the increase in the segmental mobility of the free dipole within the sisal fibril. However, the composites having alkali treated sisal fibril provide the decreasing AC conductivity which making the composites as good environment friendly electrical insulation.

Thermal characterizations

Thermal property of polyester, USFC and TSFC specimens were measured by Thermo-gravimetric analysis technique. TGA is a most important tool to study the weight loss of materials, presence of impurities and find out the percentages composition of fillers and matrix in composites. The effect of untreated and treated sisal fibril with various wt. % of loading on the degradation

temperature (D_T) of polyester composites is shown in Fig. 19. It was observed that all the composites experience weight loss in two systematic steps. At first step, all these composites show very small weight loss about 4.0 % with on onset temperature at 200°C due to the presence of moisture content in fibril^[41]. In the case of polyester resin, major weight loss about 97.3 % at 500°C. However, composites with 10-40 wt. % of untreated sisal fibrils, about 85-87 % weight loss took place at 500°C. Additionally, the unsaturated polyester resin shows about 3 % residues at 500°C. The composites which content 10-40 wt. % loading of untreated sisal fibril shows 13-15 % residue at 500°C, this may be due to condensation of lignin, cellulose and its aromatization in the presence of nitrogen atmosphere. Furthermore, the composites which content 10-40 wt. % loading of treated sisal fibril shows 15-17 % residue at 500°C. It was clearly seen that the thermal stability of TSFC was slightly higher than the USFC. Moreover, USFC and TSFC both are superior to polyester resin. Additionally, the thermal stability of composites increased with increasing loading of reinforcement filler, this may be due to better interlocking between fibril and matrix and increase the surface area after alkali treatment of sisal fibrils. The Thermo-gravimetric analyses of all samples with different % weight loss with respect to degradation temperature were observed as shown in Table-3.

Table 3. Thermogravimetric analysis data of Polyester, USFP and TSFP composites with different % weight loss.

Specimens	CD_T (°C)	D_T for 20% weight loss (°C)	D_T for 40% weight loss (°C)	D_T for 80% weight loss (°C)
Polyester	407.15	315.42	348.72	456.86
USF10P	415.33	317.83	349.38	463.98
USF20P	430.38	325.01	363.71	464.50
USF30P	435.98	328.87	366.07	464.85
USF40P	440.62	334.51	368.54	465.86
TSF10P	428.65	327.47	367.05	467.85
TSF20P	438.02	332.10	368.17	470.36
TSF30P	445.46	333.52	375.01	476.79
TSF40P	447.20	355.16	379.03	484.33

The DSC measurement was used to characterize the thermal stability of synthesized specimens of polyester, USFC and TSFC composites. Fig. 20 and Fig. 21 shows the DSC thermograms of polyester, composites with different untreated and treated sisal fibrils loadings, based on which the effects of the incorporated sisal fibrils on the polyester matrix can be explored from the aspects of both glass transition temperature (T_g) and decomposition temperature (D_i). The addition of untreated and treated sisal fibrils to the polyester matrix has no impact on the T_g at 75 °C as compared to that of pure polyester sample. However, it was noticed that the exothermic peak was

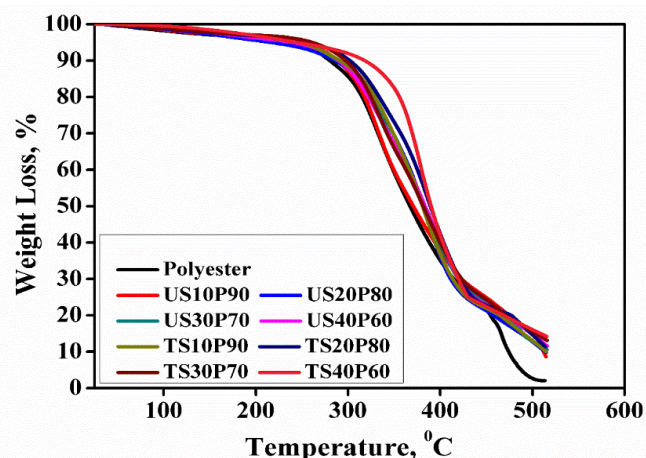


Fig. 19. TGA Thermograms of Polyester, USFC and TSFC with the variation of sisal fibril loading.

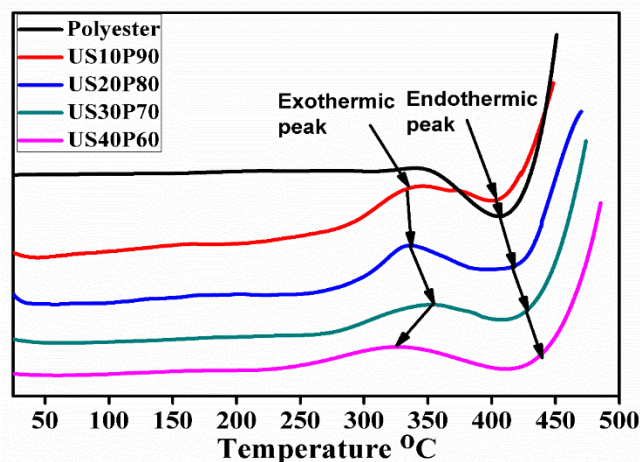


Fig. 20. DSC analysis of Polyester and USFC with the variation of sisal fibril loading.

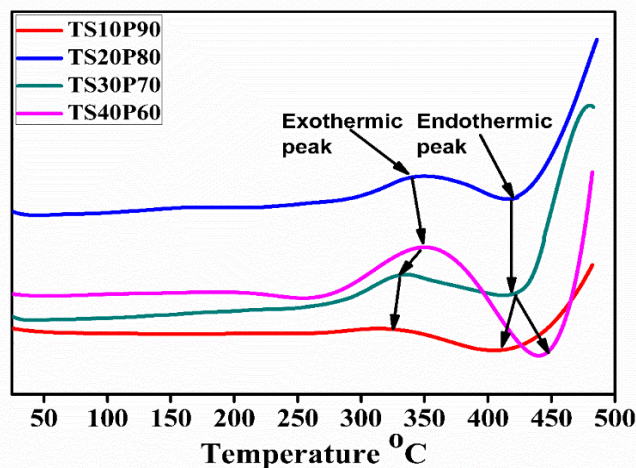


Fig. 21. DSC analysis of TSFC with the variation of sisal fibril loading.

observed between temperature range 320 to 380°C due to decomposition of hemicellulose and cellulose^[41]. The endothermic peak was also observed for decomposition of all specimens. The decomposition temperature (D_i) was measured and summarized in Table-4. The decomposition temperature of polyester was observed at 404.3°C. In case of USFC (Fig. 20) the decomposition

temperature of USF10P90, USF20P80, USF30P70 and USF40P60 were found to be 406.6, 412.8, 418.8 and 423°C respectively. The decomposition temperature of polyester resin was lower than USFC. The decomposition temperature to be affected by the loading of sisal fibrils and this could be attributed to increased molecular bonding between sisal fibril and polyester matrix resulting in enhanced the decomposition temperature of composites. On the other hand, the decomposition temperature of treated sisal fibril composites i.e. TSF10P90, TSF20P80, TSF30P70 and TSF40P60 were found to be 410, 419.8, 424 and 443.3 respectively as shown in Fig. 21. The decomposition temperature of TSF40P60 is 20 °C higher than USF40P60. This is due to the removal of hemicellulose and lignin constituent from the sisal fibril after alkali treatment^[42] and enhanced thermal strength of TSFC.

Table 4. Differential scanning calorimetry data of Polyester, USFP and TSFP composites.

Specimens	D _t (°C)
Polyester	405.98
USF10P	412.12
USF20P	421.01
USF30P	421.47
USF40P	426.71
TSF10P	421.65
TSF20P	423.15
TSF30P	424.82
TSF40P	428.80

Conclusion

Sisal fibril reinforced polyester composites with varying fibril loading were developed for electrical insulation purpose. Sisal fibrils were extracted from sisal fibre and these fibrillated fine fibrils were used for reinforcement. Alkali treatment showed improved surface characteristics of sisal fibril to make composites. The SEM micrographs clearly show that the composites exhibit excellent interlocking between fibril and matrix with treated fibril and higher loading. The composites showed excellent electrical, mechanical and thermal properties. Excellent electrical properties with NaOH treated sisal fibril composites were observed and results were superior in higher frequency region. The value of ϵ' for 10 wt. % alkali treated fibril composite was observed as 2.09 at 20×10^3 Hz confirming that the composite material exhibits good electrical insulation. A change in fibril loading from 10 to 40 wt. % showed 47.71% increase in tensile strength i.e. from 49.94 to 73.77 MPa. Similarly flexural as well as impact strength also increased by 58.19% and 136.86% respectively. The alkali treatment with 5% solution showed improved results with improvement up to 44.30% in tensile strength. Thermo-gravimetric analysis of TSFC

shows lower weight loss (83%) as compare to USFC (87%) and Polyester (97%). respectively. The decomposition temperature of TSFC is 20 °C higher than USFC and 40°C higher than polyester. Different micro-mechanical models were applied to sisal fibril polyester composites to predict the Young's modulus. Nielson-Chen model was found fairly accurate in predicting the elastic properties. This investigation provides scientific information and confirms that sisal fibril based composites exhibit a balanced set of characteristic including mechanical, Thermal and electrical insulation for being considered environment friendly electrical insulating material.

Acknowledgements

The Author Subhash Nimanpure is highly thankful to UGC, New Delhi for granting Rajiv Gandhi National Fellowship under which the present work was carried out. All Authors are highly thankful to Director CSIR-Advanced Materials and Processes Research Institute, Bhopal for encouraging R&D work in this area and persuasion.

Author's contributions

S. Nimanpure fabricated composites and analyzed the results with the help of SAR Hashmi. The mechanical characterization was done by S. Nimanpure and A. Naik. The electrical and thermal characterization was done by S. Nimanpure and A. Nigrawal. The micromechanical models were applied by R. Kumar. The SEM and FESEM study done by H.N Bhargaw and S. Nimanpure. S. Nimanpure wrote the manuscript with the help of SAR Hashmi. The whole work was supervised by SAR Hashmi.

References

- Wang, W.; Huang, G; *Materials & Design* **2009**, *30*, 2741.
DOI: [10.1016/j.matdes.2008.11.002](https://doi.org/10.1016/j.matdes.2008.11.002)
- Akil, H.; Omar, M.; Mazuki, A.; Safiee, S.; Ishak, Z. M. ; Bakar, A. A; *Materials & Design* **2011**, *32*, 4107.
DOI: [10.1016/j.matdes.2011.04.008](https://doi.org/10.1016/j.matdes.2011.04.008)
- Amada, S.; Untao, S; *Composites Part B: Engineering* **2001**, *32*, 451.
DOI: [10.1016/S1359-8368\(01\)00022-1](https://doi.org/10.1016/S1359-8368(01)00022-1)
- Goda, K.; Sreekala, M.; Gomes, A.; Kaji, T.; Ohgi, J; *Composites Part A: Applied Science and Manufacturing* **2006**, *37*, 2213.
DOI: [10.1016/j.compositesa.2005.12.014](https://doi.org/10.1016/j.compositesa.2005.12.014)
- Threepopnatkul, P.; Kaerkitcha, N.; Athipongarporn, N; *Composites Part B: Engineering* **2009**, *40*, 628.
DOI: [10.1016/j.compositesb.2009.04.008](https://doi.org/10.1016/j.compositesb.2009.04.008)
- Li, Y.; Pickering, K.L; *Composites Science and Technology* **2008**, *68*, 3293.
<https://doi.org/10.1016/j.compscitech.2008.08.022>
- Asasutjarit, C.; Charoenvai, S.; Hirunlabh, J.; Khedari, J; *Composites Part B: Engineering* **2009**, *40*, 633.
DOI: [10.1016/j.compositesb.2009.04.009](https://doi.org/10.1016/j.compositesb.2009.04.009)
- Suppakarn, N.; Jarukumjorn, K; *Composites Part B: Engineering* **2009**, *40*, 613.
DOI: [10.1016/j.compositesb.2009.04.005](https://doi.org/10.1016/j.compositesb.2009.04.005)
- Le Duigou, A.; Pillin, I.; Bourmaud, A.; Davies, P.; Baley, C; *Composites Part A: Applied Science and Manufacturing* **2008**, *39*, 1471.
DOI: [10.1016/j.compositesa.2008.05.008](https://doi.org/10.1016/j.compositesa.2008.05.008)
- Corrales, F.; Vilaseca, F.; Llop, M.; Girones, J.; Mendez, J.; Mutje, P; *Journal of Hazardous Materials* **2007**, *144*, 730.
DOI: [10.1016/j.jhazmat.2007.01.103](https://doi.org/10.1016/j.jhazmat.2007.01.103)
- Luo, S.; Netravali, A; *Polymer Composites* **1999**, *20*, 367.
DOI: [10.1002/pc.10363](https://doi.org/10.1002/pc.10363)
- Torres, F.; Cubillas, M; *Polymer Testing* **2005**, *24*, 694.
DOI: [10.1016/j.polymertesting.2005.05.004](https://doi.org/10.1016/j.polymertesting.2005.05.004)
- Bledzki, A.; Gassan, J; *Progress in polymer science* **1999**, *24*, 221.
DOI: [10.1016/S0079-6700\(98\)00018-5](https://doi.org/10.1016/S0079-6700(98)00018-5)

14. Gassan, J.; Bledzki, A.K; *Composites Science and Technology* **1999**, *59*, 1303.
DOI: [10.1016/S0266-3538\(98\)00169-9](https://doi.org/10.1016/S0266-3538(98)00169-9)
15. Hashmi, S.A.R.; Naik, A.; Chand, N.; Sharma, J.; Sharma, P; *Composite Interfaces* **2011**, *18*, 671.
DOI: [10.1163/156855412x626252](https://doi.org/10.1163/156855412x626252)
16. Alavudeen, A.; Rajini, N.; Karthikeyan, S.; Thiruchitrabalam, M.; Venkateshwaren, N; *Materials & Design* **2015**, *66*, 246.
DOI: [10.1016/j.matdes.2014.10.067](https://doi.org/10.1016/j.matdes.2014.10.067)
17. Mylsamy, K.; Rajendran, I; *Journal of Reinforced Plastics and composites* **2010**, *29*, 2925.
DOI: [10.1177/0731684410362817](https://doi.org/10.1177/0731684410362817)
18. Mylsamy, K.; Rajendran, I; *Materials & Design* **2011**, *32*, 4629.
DOI: [10.1016/j.matdes.2011.04.029](https://doi.org/10.1016/j.matdes.2011.04.029)
19. Ghali, L.H.; Aloui, M.; Zidi, M.; Daly, H.B.; Msahli S.; Sakli, F; *BioResources* **2011**, *6*, 3836.
http://ojs.cnr.ncsu.edu/index.php/BioRes/article/view/BioRes_06_4_3836_Ghali_AZBMS_Chem_Modl_Luffa_Cylindrica.
20. Aziz, S.H.; Ansell, M.P; *Composites Science and Technology* **2004**, *64*, 1231.
DOI: [10.1016/j.compscitech.2003.10.002](https://doi.org/10.1016/j.compscitech.2003.10.002)
21. Aziz, S.H.; Ansell, M.P.; Clarke, S.J.; Panteny, S.R; *Composites Science and Technology* **2005**, *65*, 525.
<https://doi.org/10.1016/j.compscitech.2004.08.005>
22. Singh, B.; Gupta, M.; Verma, A; *Polymer Composites* **1996**, *17*, 910.
DOI: [10.1002/pc.10684](https://doi.org/10.1002/pc.10684)
23. Jacob, M.; Varughese, K.; Thomas, S; *Journal of Materials Science* **2006**, *41*, 5538.
DOI: [10.1007/s10853-006-0298-y](https://doi.org/10.1007/s10853-006-0298-y)
24. Cabral, H.; Cisneros, M.; Kenny, J.; Vazquez, A.; Bernal, C; *Journal of composite materials* **2005**, *39*, 51.
DOI: [10.1177/0021998305046434](https://doi.org/10.1177/0021998305046434)
25. Pothan, L.A.; George, C.N.; Jacob, M.; Thomas, S. *Journal of composite materials* **2007**, *41*, 2371.
DOI: [10.1177/0021998307075456](https://doi.org/10.1177/0021998307075456)
26. Paul, A.; Joseph, K.; Thomas, S; *Composites Science and Technology* **1997**, *57*, 67.
DOI: [10.1016/S0266-3538\(96\)00109-1](https://doi.org/10.1016/S0266-3538(96)00109-1)
27. Lv, J.; Zeng, D.M.; Wei, C; *Adv Polym Technol.* **2015**, *34*, 1.
DOI: [10.1002/adv.21483](https://doi.org/10.1002/adv.21483)
28. Paluvai, N.R.; Mohanty, S.; Nayak, S.K; *Polymer Composites* **2016**, *37*, 2832.
DOI: [10.1002/pc.23480](https://doi.org/10.1002/pc.23480)
29. Rao, K.M.M.; Rao, K.M.; Prasad, A.V.R; *Materials & Design* **2010**, *31*, 508.
DOI: [10.1016/j.matdes.2009.06.023](https://doi.org/10.1016/j.matdes.2009.06.023)
30. Hashmi, S.A.R.; Chand N.; Naik, A; *India Patent Journal No. 02/2011*, **2011**.
31. Gomes, A.; Goda, K.; Ohgi, J; *JSME International Journal Series A Solid Mechanics and Material Engineering* **2004**, *47*, 541.
Doi:10.1299/jsmea.47.541
32. Hinrichsen, G.; Mohanty, A.; Khan, M; *Composites Part A: Applied Science and Manufacturing* **2000**, *31*, 143.
DOI: [10.1016/S1359-835X\(99\)00057-3](https://doi.org/10.1016/S1359-835X(99)00057-3)
33. Ray, D.; Sarkar, B.K; *Journal of applied polymer science* **2001**, *80*, 1013.
DOI: [10.1002/app.1184](https://doi.org/10.1002/app.1184)
34. Cao, Y.; Shibata, S.; Fukumoto, I; *Composites Part A: Applied Science and Manufacturing* **2006**, *37*, 423.
DOI: [10.1016/j.compositesa.2005.05.045](https://doi.org/10.1016/j.compositesa.2005.05.045)
35. Jones, R.M; *Mechanics of composite materials*, CRC press **1998**.
36. Halpin, J; *Journal of composite materials* **1969**, *3*, 732.
DOI: [10.1177/002199836900300419](https://doi.org/10.1177/002199836900300419)
37. Affdl, J.C.H.; Kardos, J.L; *Polymer Engineering & Science* **1969**, *16*, 344.
DOI: [10.1002/pen.760160512](https://doi.org/10.1002/pen.760160512)
38. Bader, M.G.; Bowyer, W.H; *Composites* **1973**, *4*, 150.
DOI: [10.1016/0010-4361\(73\)90105-5](https://doi.org/10.1016/0010-4361(73)90105-5)
39. Manera, M; *Journal of composite materials* **1977**, *11*, 235.
DOI: [10.1177/002199837701100208](https://doi.org/10.1177/002199837701100208)
40. Singha, A.S.; Rana, A.K.; Jarial, R.K; *Materials & Design* **2013**, *51*, 924.
DOI: [10.1016/j.matdes.2013.04.035](https://doi.org/10.1016/j.matdes.2013.04.035)
41. Adriana, M.A.M.; Martin, R.; Mattoso, Luiz H.C.; Silva, Odilon R.R.F; *Polímeros* **2009**, *19*, 40.
DOI: [10.1590/S0104-14282009000100011](https://doi.org/10.1590/S0104-14282009000100011)
42. Ray, D.; Sarkar, B.K.; Basak, R.K.; Rana, A.K; *Journal of applied polymer science* **2002**, *85*, 2594.
DOI: [10.1002/app.10934](https://doi.org/10.1002/app.10934)